Synthesis of functional polypyrrole/prussian blue and polypyrrole/Ag composite microtubes by using a reactive template

2007 Nanotechnology 18 195603

(http://iopscience.iop.org/0957-4484/18/19/195603)

IOP PUBLISHING NANOTECHNOLOGY
Nanotechnology **18** (2007) 195603 (7pp) doi:10.1088/0957-4484/18/19/195603

Synthesis of functional polypyrrole/prussian blue and polypyrrole/Ag composite microtubes by using a reactive template

Xiaomiao Feng, Zhengzong Sun, Wenhua Hou[1] and Jun-Jie Zhu[1]

Key Laboratory of Mesoscopic Chemistry, Key Laboratory of Analytical Chemistry for Life Science, School of Chemistry and Chemical Engineering, Nanjing University, Nanjing 210093, People's Republic of China

E-mail: whou@nju.edu.cn and jjzhu@nju.edu.cn

Received 25 January 2007, in final form 2 March 2007
Published 17 April 2007
Online at stacks.iop.org/Nano/18/195603

Abstract
Polypyrrole (PPy)/PB and PPy/Ag composite microtubes were synthesized in one pot by using methyl orange (MO) as a reactive self-degraded template. In contrast to reported conventional template approaches, the MO template did not need to be removed after polymerization. The formation mechanism, structural characteristics, conductivity, and electrochemical properties of the obtained PPy/PB and PPy/Ag microtubes are reported.

1. Introduction

The ability to control the size and morphology of materials is an important factor for defining properties such as the electronic band gap [1] and conductivity or light emission efficiency [2]. Conducting polymers with tubular structure have recently attracted considerable attention because of their unique properties and promising applications in materials science and nanodevices [3]. Template-assisted synthesis is an efficient, controllable, and conventional route to fabricate these materials, especially nano/microstructured conducting polymers. To date, a series of nano/microstructured conducting polymers has been prepared using this method. For example, 'hard templates' such as porous polycarbonate films [4], fibrillar V_2O_5 [5], and porous alumina [6] or 'soft templates' such as reverse microemulsion [7, 8], micelles [9, 10], and liquid crystalline phases [11] have been reported to prepare polypyrrole (PPy) or polyaniline nanotubes and nanofibres. The main advantage of the template synthesis method is that the length and diameter of the products can be controlled by the selected porous membrane. However, the removal of the template is tedious when hard templates are used.

Synthesizing composite materials is an effective way to combine the features of different materials and tailor the properties to achieve the desired material performance. PPy stands out because of its high conductivity, good environmental stability, and its large variety of applications [12, 13]. Composites containing PPy and many inorganic nanoparticles such as AgCl [14], Ag [15], Au [5, 16], SWCT [17], CuS [18], and prussian blue (PB) [19, 20] have been synthesized. Among those inorganic materials, PB nanoparticles have received much attention and play many important roles in the fields of magnetic molecules [21], electrochromic devices [22], and rechargeable batteries [23] owing to their interesting electrochemical, photophysical, and magnetic properties. Especially in the field of electroanalytical chemistry, PB nanoparticles attract the attention of the biosensor community [24, 25]. In addition, much effort has been focused on the preparation of noble metal (such as Au and Ag) and conducting polymer composites because of their superior performance as nanocircuits, nanodevices, and nanosensors [26, 27]. Although PPy/PB composite films [19, 28, 29] and PPy/Ag composites [30–32] are well documented, the composite nanotubes are rarely reported. Pyrrole monomer can be oxidized by potassium ferricyanide (KHCF) [33] or silver nitrate to form PPy and, PB or Ag [31, 32], respectively. This suggests that PPy/PB and PPy/Ag composite nanostructures can be prepared in one step by selecting an appropriate surfactant or stabilizer.

Lu *et al* [34] synthesized pure PPy nanotubes by using methyl orange (MO) as the template and $FeCl_3$ as the oxidant.

[1] Authors to whom any correspondence should be addressed.

In this paper, we report the synthesis of PPy/PB and PPy-coated Ag composite microtubes prepared by using MO as the template in the presence of KHCF and silver nitrate as the oxidants, respectively. In contrast to the conventional template, the MO does not need the subsequent template-removal treatment because the obtained PPy can be doped by MO. During the formation process of PPy/Ag, ultraviolet-light was introduced in order to improve the reaction rate and distribution level of Ag nanoparticles. Here, MO played three important roles in the experiments: template, dopant, and stabilizer, resulting in the formation of PPy-coated Ag composite microtubes. The PPy/PB composite microtubes were also immobilized on the surface of a glassy carbon electrode and applied to construct a sensor; it showed one well-defined pair of redox peaks and a dramatic catalysis for the reduction of H_2O_2. The PPy/Ag composite microtubes showed excellent electrochemical activity. The formation mechanism, structural characteristics, and conductivity of the obtained PPy/PB and PPy/Ag microtubes are discussed.

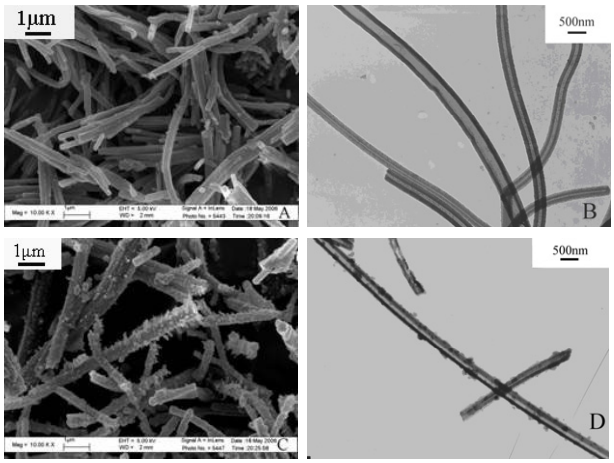

Figure 1. SEM and TEM images of PPy/PB composite microtubes synthesized at different concentrations of KHCF. Synthetic conditions: pyrrole 105 μl, MO 0.05 g, [Py]/[KHCF] 1:2 (A), (B) and 1:10 (C), (D), solvent hydrochloric acid, reaction time 24 h, room temperature.

2. Experimental details

2.1. Materials

Pyrrole monomer (Aldrich) was distilled under reduced pressure. Methyl orange (MO), potassium ferricyanide (KHCF), silver nitrate ($AgNO_3$), and hydrochloric acid (HCl) were purchased from Shanghai Chemical Reagent Co. and used as received without further treatment.

2.2. Preparation of PPy/PB composite microtubes

0.05 g of MO was dispersed in 20 ml of pH 4 HCl aqueous solution. Pyrrole monomer (105 μl) was added, and the mixture was stirred for several minutes. 10 ml of pH 4 HCl aqueous solution of KHCF as an oxidant was dropped into the above mixture under stirring at room temperature. The molar ratio of pyrrole to KHCF ([Py]/[KHCF]) was 1:2 or 1:10 (pyrrole: 1.5 mmol). A small quantity of $FeCl_3$ was added to promote the formation of PB after several hours. The reaction was allowed to proceed for 24 h. After that, the precipitate was centrifuged and washed with distilled water and ethanol. The final product was dried in vacuum at 40 °C for 24 h.

2.3. Preparation of PPy/Ag composite microtubes

0.05 g of MO was dispersed in 20 ml of distilled water. 5 ml of $AgNO_3$ (0.24 g) aqueous solution was added to the above solution and a red precipitate was formed immediately. Pyrrole monomer (105 μl) was added after stirring for several minutes. The mixture was irradiated by UV-light (500 W, $\lambda = 365$ nm) under stirring. After 2 h, the UV-light was removed and the reaction was continued for 10 h. The precipitate was centrifuged and washed with distilled water and ethanol. The final product was dried in vacuum at 40 °C for 24 h.

2.4. Characterization

The morphologies of the PPy/PB and PPy/Ag tubular structures were observed using a scanning electron microscope (SEM, LEO1530VP) and a transmission electron microscope (TEM, JEOL JEM-200CX). Powder x-ray diffraction patterns (XRD) were taken on a Philip-X'Pert x-ray diffractometer with a Cu Kα x-ray source. Fourier-transform infrared (FTIR) spectroscopy measurements were performed on a Bruker Fourier transform spectrometer model VECTOR22 using KBr pressed discs. X-ray photoelectron spectroscopic (XPS) analysis was carried out on a ESCALAB MK II x-ray photoelectron spectrometer. Conductivity was measured using a four-probe method on a WR-2B digital multimeter at room temperature using compressed pellets of powders. For each value reported, at least three measurements were averaged. Electrochemical experiments were conducted with a CHI660B workstation (Shanghai Chenhua, Shanghai) in a three-electrode system. All electrochemical experiments were performed in a cell containing 10.0 ml of phosphate buffer solution (PBS, 0.1 M, pH 6) at room temperature and using a coiled platinum wire as the auxiliary, a saturated calomel electrode (SCE) as the reference, and the PPy/PB modified glassy carbon electrode (GCE) as the working electrode. All experimental solutions were deaerated by bubbling highly pure nitrogen for 20 min, and a nitrogen atmosphere was kept over the solutions during the measurements.

3. Results and discussion

3.1. Formation mechanism

PPy/PB and PPy/Ag composite microtubes were successfully synthesized via a facile one-step method in the presence of MO. Typical SEM and TEM images of PPy/PB composite microtubes synthesized at different molar ratios of pyrrole to KHCF ([Py]/[KHCF]) are shown in figure 1. The diameters and lengths of the resulting microtubes are 300–500 nm and 1–10 μm, respectively. Figures 1(A) and (B) show the SEM and TEM images of the resulting product prepared at a [Py]/[KHCF] ratio of 1:2. As can be seen, most of the obtained microtubes with smooth walls are due to the formation of pure PPy microtubes. However, when [Py]/[KHCF] is increased

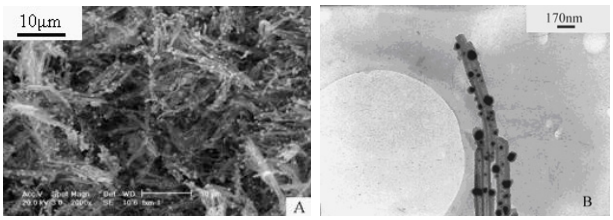

Figure 2. SEM (A) and TEM (B) images of PPy/Ag composite microtubes. Synthetic conditions: pyrrole 105 μl, MO 0.05 g, $AgNO_3$ 0.24 g, solvent distilled water, UV irradiation time 2 h, room temperature.

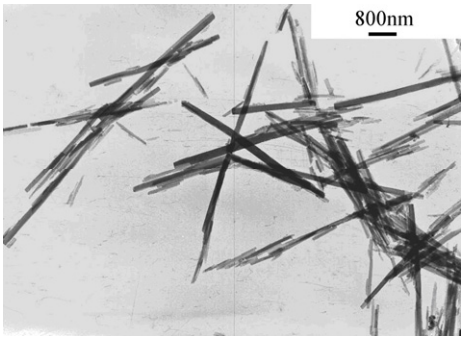

Figure 3. TEM image of MO higher oligomers.

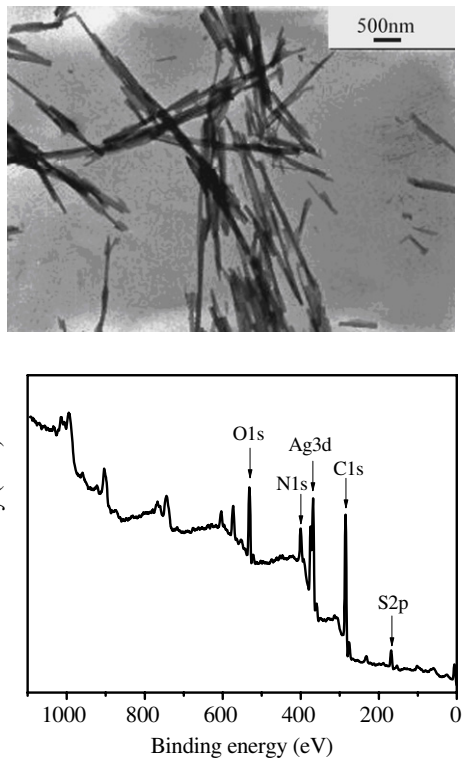

Figure 4. TEM image and XPS spectrum of MO–$AgNO_3$.

from 1:2 to 1:10, PPy/PB composite microtubes can be formed. The outside particles in figure 1(C) and the corresponding spots in figure 1(D) are PB nanoparticles. Figure 2 shows typical SEM and TEM images of PPy/Ag composite microtubes. The diameters and lengths of the resulting microtubes are 80–150 nm and 1–12 μm, respectively. The outside particles in figure 2(A) and the dark spots in figure 2(B) are Ag nanoparticles. It can be seen from figure 2(B) that Ag nanoparticles with sizes in the range of 20–80 nm are dispersed without aggregation. It should be noted that the Ag nanoparticles are wrapped by a layer of PPy matrix, which can be seen from the TEM images (figure 2(B)). The diameter of the PPy/Ag microtubes is smaller than that of the PPy/PB microtubes, which may be caused by the different reaction mechanism.

During the process for the formation of PPy/PB and PPy/Ag composite microtubes, MO played an important role. Without MO, the tube-like structure could not be formed. It is well known that MO with a planar hydrophobic section and hydrophilic end group ($-SO_3^-$) is water soluble and has anionic characteristics in aqueous solution. Being different from some large organic dopant anions such as salicylic acid, MO has no surfactant characteristic because of the absence of the crucial micelle concentration. In aqueous solution at 25 °C, MO can dimerize at low concentration and form higher oligomers at high concentration [35]. Furthermore, MO can form higher oligomers with different numbers of MO monomers in acidic conditions. Figure 3 shows the one-dimensional fibre-like structure of the MO oligomer precipitate obtained by adding 0.05 g MO into 30 ml of pH 4 HCl. The fibres with different diameters and lengths suggest the formation of higher oligomers with different numbers of MO monomers. On the other hand, it is known that complexation can be obtained between organic compounds such as phenol or dye and flocculent such as Al^{3+} or Fe^{3+} [36]. In our work, $AgNO_3$ can be considered to act as a flocculent. A red precipitate appeared immediately when $AgNO_3$ was added to the MO aqueous solution. As shown in figure 4, the red precipitate has a one-dimensional fibrillar structure and the composition, determined by XPS, is MO–$AgNO_3$ with enriched $AgNO_3$ on the surface.

A possible mechanism for the formation of PPy/PB and PPy/Ag composite microtubes is shown in scheme 1. As far as the PPy/PB is concerned, firstly, pyrrole monomer can be adsorbed on the MO fibre by electrostatic effects because there are many electronegative $-SO_3^-$ groups on the surface. When the oxidant was added, pyrrole *in situ* polymerizes along the one-dimensional fibre. $[Fe(CN)_6]^{4-}$ will be formed when KHCF induces the polymerization of pyrrole. At the same time, free Fe^{3+} and Fe^{2+} ions were generated *in situ* in the reaction mixture. Subsequently, when free Fe^{3+} or Fe^{2+} ions meet $[Fe(CN)_6]^{4-}$ or $[Fe(CN)_6]^{3-}$, different reactions can take place, resulting in the formation of PB. In a strongly acidic solution, the formation of both PB and PPy proceed at comparable rates [37]. Moreover, the strongly acidic medium favours the decomposition of the hexacyanoferric/ferrous complexes. Therefore, the formation rate of PPy was higher than that of PB when the concentration of HCl was 10^{-4} M. On the other hand, PB particles will lose their negative charge at pH lower than 2.5, which is not propitious to the formation of PPy/PB composite microtubes [38, 39]. The pH value was selected as 4, to assure a relative high reaction rate and to protect the PB nanoparticles from losing their negative charge.

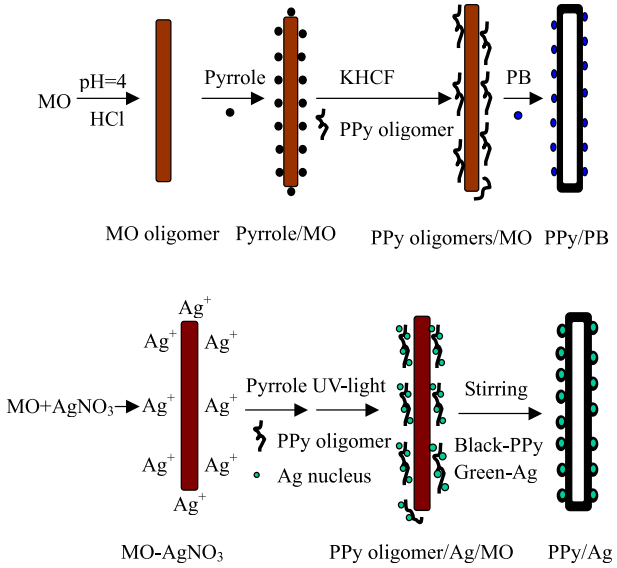

Scheme 1. Scheme of the formation of PPy/PB and PPy/Ag composite microtubes.

(This figure is in colour only in the electronic version)

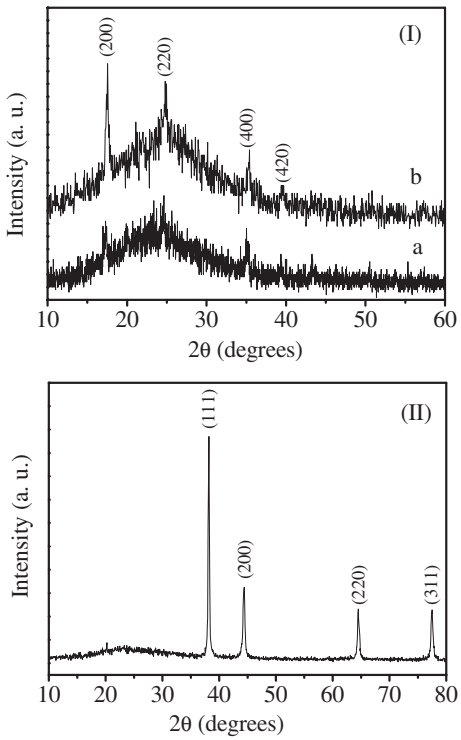

Figure 5. XRD patterns of PPy/PB (I) and PPy/Ag (II) composite microtubes. Synthetic conditions of PPy/PB (1) and PPy/Ag (2): (1) pyrrole 105 μl, MO 0.05 g, [Py]/[KHCF] 1:2 (a) and 1:10 (b), solvent hydrochloric acid, reaction time 24 h, room temperature; (2) pyrrole 105 μl, MO 0.05 g, $AgNO_3$ 0.24 g, solvent distilled water, UV irradiation time 2 h, room temperature.

When the polycationic PPy meets the electronegative PB, the two materials can effectively assemble composite microtubes by electrostatic attraction. At the same time, PPy is doped by MO and MO higher oligomers themselves degrade, resulting in the formation of PPy/PB microtubes [34]. The PB content is very low in the composite when [Py]/[KHCF] is 1:2 because the majority of the KHCF is used to induce the pyrrole monomer polymerization. Therefore, most of the obtained microtubes have smooth walls. When [Py]/[KHCF] is increased to 1:10, there is enough KHCF to induce the pyrrole polymerization and to act as a resource for the formation of PB, so the PPy/PB composite microtubes can be formed. The formation mechanism of PPy/Ag composite microtubes is different from that of PPy/PB, though MO also plays the key role. The fibrillar MO–$AgNO_3$ with enriched $AgNO_3$ on the surface acts as a template and the reaction is carried out in distilled water during the fabrication of PPy/Ag composite microtubes. When the mixture containing pyrrole and MO–$AgNO_3$ is irradiated by UV-light, pyrrole *in situ* polymerizes along the one-dimensional fibre and a Ag nucleus is formed on the MO–$AgNO_3$ fibre surface at the same time. The complex MO–$AgNO_3$ template itself degrades automatically due to the reduction of oxidizing cations and MO can dope PPy during polymerization. Ag–O coordination can be formed between MO and Ag nanoparticles on the surface of the silver [40]. It is well known that specific functional groups such as –CONH–, $-SO_4^-$, and –C=O groups can be used to induce coating during the precipitation and surface reactions on the cores [41–43]. Herein, MO acts as a useful stabilizer to promote a strong interaction between the Ag nanoparticles and the PPy matrix. The doping MO may provide active sites on the Ag so as to induce the growing polycationic PPy chains to complete the coating of PPy layers, resulting in the formation of PPy-coated Ag composite microtubes. MO has played three important roles in this experiment: template, dopant, and stabilizer. In particular, UV-light has an important effect on the reaction rate and the distribution level of Ag nanoparticles. The reaction was finished in 48 h and the size of the Ag nanoparticles was in the micrometre range without UV-light. Silver ion as an oxidant, which has a standard reductive potential similar to Fe^{3+}, fails to produce polypyrrole within 12 h [44]. A possible reason for this is that the reaction, although thermodynamically favourable, is kinetically very slow for this metal. UV-light was used to induce the reaction of pyrrole and silver nitrate, and the whole reaction was finished in 2 h and the size of the Ag nanoparticles was less than 100 nm. The UV-light was removed after 2 h and the reaction was continued for 10 h to promote complete polymerization of pyrrole. The molar ratio of pyrrole to silver nitrate has less effect on the morphology of the resultant sample. During the process, the fibrillar reactive template directed the growth and formation of PPy/PB and PPy/Ag microtubular structures. Therefore, MO can act as a template and a dopant at the same time. In contrast to the conventional template, the MO does not need subsequent template-removal treatment.

3.2. Structural characteristics

The x-ray diffraction (XRD) patterns of the PPy/PB prepared at different values of [Py]/[KHCF] and PPy/Ag are shown in figure 5. XRD measurement confirms the presence of PB and Ag in the PPy/PB and PPy/Ag composite microtubes, respectively. As shown in figure 5(I), the distinct reflection centred at a 2θ value of 25° is characteristic of

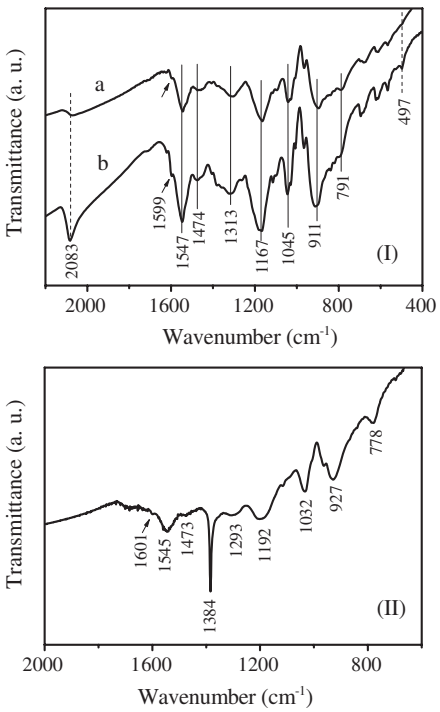

Figure 6. FTIR of PPy/PB (I) and PPy/Ag (II) composite microtubes. Synthetic conditions of PPy/PB (1) and PPy/Ag (2): (1) pyrrole 105 μl, MO 0.05 g, [Py]/[KHCF] 1:2 (a) and 1:10 (b), solvent hydrochloric acid, reaction time 24 h, room temperature; (2) pyrrole 105 μl, MO 0.05 g, $AgNO_3$ 0.24 g, solvent distilled water, UV irradiation time 2 h, room temperature.

the doped PPy [45]. Another four diffraction peaks at $2\theta = 17.5°, 24.8°, 35.4°$, and $39.5°$ correspond to Bragg's reflections from the (200), (220), (400) and (420) planes of PB and are in good agreement with the reported data (JCPDS File No. 730687), showing the existence of PB nanoparticles in the PPy/PB composite. Moreover, with the increase in KHCF content, the relative diffraction peak intensity for PB is increased, indicating that the percentage of PB in the composite is elevated. In the XRD of PPy/Ag (figure 5(II)), besides the broad band of PPy, four strong diffraction peaks centred at $2\theta = 38.2°, 44.4°, 64.5°$, and $77.5°$ are due to Bragg's reflections from the (111), (200), (220) and (311) planes of Ag and are in accordance with the reported data, confirming the presence of Ag [46].

The molecular structures of the PPy/PB and PPy/Ag composite microtubes were characterized by FTIR. The FTIR spectrum of the PPy/PB composite is shown in figure 6(I). It is clearly seen that the characteristic PPy peaks are located at 1547 and 1474 cm^{-1}, due to the pyrrole ring-stretching and the conjugated C–N stretching mode, respectively [47, 48]. The peaks at 1313 and 1045 cm^{-1} are related to the in-plane vibration of =C–H, 1167 cm^{-1} is assigned to the C–N stretching mode, and 791 cm^{-1} is attributable to C–H wagging vibration [49]. In addition, the band at 2083 cm^{-1} corresponds to the stretching vibration of the CN group [50], and the absorption band at 497 cm^{-1} is due to the formation of Fe^{II}–CN–Fe^{III} [51], which indicates the presence of PB. Moreover, the shoulder peak at 1599 cm^{-1} is attributable to the stretching vibration mode of the benzene ring in the MO molecule. This indicates that the prepared PPy is doped by MO. The relative vibration intensity for PB increases with the KHCF content, indicating that the percentage of PB in the composite is elevated. This result is in accordance with the XRD results. The typical characteristic peaks of PPy and the shoulder peak of MO all appear in the FTIR spectrum of the PPy/Ag composite (figure 6(II)). Furthermore, a very strong absorption band assignable to NO_3^- is observed at 1384 cm^{-1}. This suggests that the obtained PPy in the PPy/Ag composite microtubes is not only doped by MO but is also doped by NO_3^-.

XPS was also used to characterize the samples in a wide scan (figure 7(A)). Curve (a) shows the composition of the obtained PPy/PB composite microtubes, (C, N, O, S, Cl, and Fe), indicating that the PPy is doped by MO and Cl^-. At the same time, the formation of PB nanoparticles is also confirmed. K^+ was not detected, indicating that the obtained PB is insoluble. As we known, there are two forms of PB crystals: the so-called insoluble PB with the molecular formula $Fe_4^{III}[Fe^{II}(CN)_6]_3$ and the soluble $KFe^{III}[Fe^{II}(CN)_6]$ [52]. The doping level of MO and Cl^- is 8% and 3%, calculated according to the molecular formulae of PPy, PB, and MO. Compared to the XPS of PPy/PB, a new peak corresponding to the Ag 3d is observed at 368.4 eV in curve (b). The doping level of MO and NO_3^- in the PPy is 13% and 27%, respectively. Further studies on the high-resolution XPS of the Fe 2p region of the PPy/PB indicate that Fe exists in both Fe(II) (708.5 eV) and Fe(III) (710.9 eV) states and their atomic ratio is 0.71, which is near 0.75, as shown in figure 7(B) [53]. In the high-resolution XPS of the N 1s region of the PPy/PB (figure 7(C)), there is an intense peak at 399.8 eV corresponding to the pyrrole nitrogen (–NH–) and a high binding energy (401.9 eV) tail characteristic of positively charged nitrogen [54]. In addition, the distinct peak at 397.6 eV ascribes to the nitrogen in PB [53]. The atomic ratio of pyrrole nitrogen and positively charged nitrogen to nitrogen in PB is 2.6. These high-resolution XPS results are further confirmation of the formation of PPy and PB.

3.3. Conductivities

The conductivity of PPy/PB is 4 S cm^{-1} when the molar ratio of [Py]/[KHCF] is 1:2. However, with the increase in KHCF content, the conductivity of PPy/PB decreases from 4 to 1 S cm^{-1}. The conductivity of PPy/PB will decrease if the content of PB increases because PB is a nonconductor. The amount of PB increases with the increase in KHCF content, leading to a decrease in the conductivity of PPy/PB. The conductivity of PPy/Ag composite microtubes is 10 S cm^{-1}, which is higher than that of PPy/PB. Since silver is a conductor, it is beneficial for improving the conductivity of PPy when PPy is combined with silver. Therefore, when PPy is combined with silver, the conductivity of PPy will be enhanced. In addition, the PPy in the PPy/Ag composite is doped by a large amount of MO and NO_3^-, leading to its high conductivity.

3.4. Electrochemical properties

It is well known that PB bears good electrochemical behaviour and has been widely applied to the field of chemically modified electrodes. Furthermore, conductive PPy with high conductivity can improve charge transfer. On the basis of

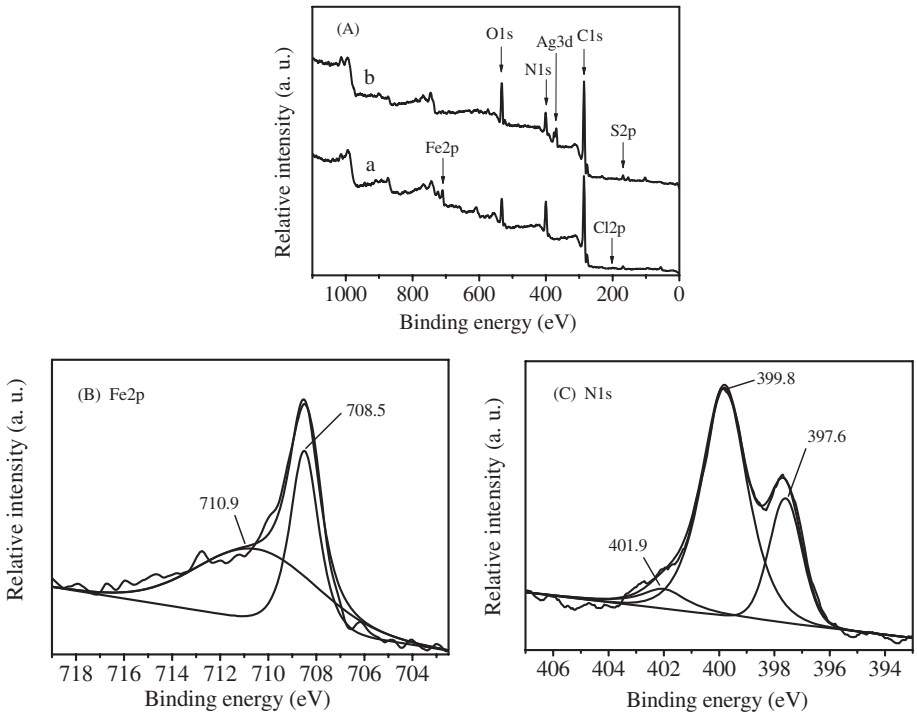

Figure 7. (A) XPS spectra of PPy/PB (a) and PPy/Ag (b) composite microtubes; (B) and (C) are the XPS data of the Fe 2p and N 1s regions of the PPy/PB, respectively. Synthetic conditions of PPy/PB (1) and PPy/Ag (2):(1) pyrrole 105 μl, MO 0.05 g, [Py]/[KHCF] 1:10, solvent hydrochloric acid, reaction time 24 h, room temperature; (2) pyrrole 105 μl, MO 0.05 g, $AgNO_3$ 0.24 g, solvent distilled water, UV irradiation time 2 h, room temperature.

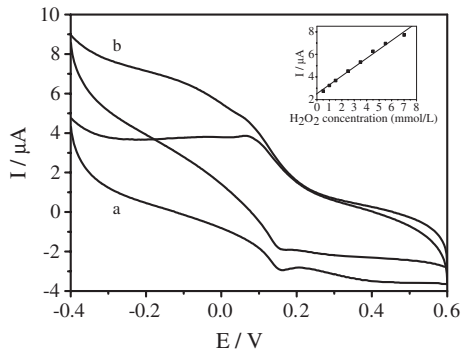

Figure 8. Cyclic voltammograms of PPy/PB composite microtube modified GCE immersed in pH 6 PBS without (a) and with (b) 7.0 mM H_2O_2 at 100 mV s^{-1}. The inset shows the changes in the current response under different concentrations of H_2O_2. Synthetic conditions: pyrrole 105 μl, MO 0.05 g, [Py]/[KHCF] 1:10, solvent hydrochloric acid, reaction time 24 h, room temperature.

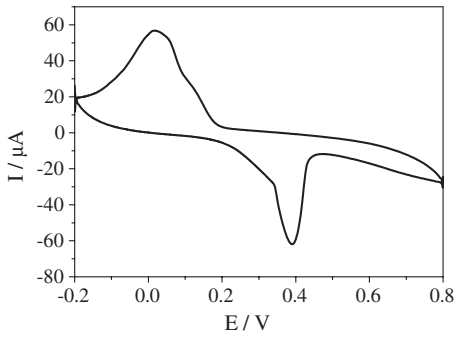

Figure 9. Cyclic voltammograms of PPy/Ag composite microtube modified GCE immersed in pH 6 PBS at 100 mV s^{-1}. Synthetic conditions: pyrrole 105 μl, MO 0.05 g, $AgNO_3$ 0.24 g, solvent distilled water, UV irradiation time 2 h, room temperature.

the excellent electrochemical properties of PB and the high conductivity of PPy, PPy/PB composites were immobilized on the surface of a glassy carbon electrode and were applied to construct a sensor. In the potential range of 0.6 and −0.4 V, the cyclic voltammograms of a PPy/PB modified electrode in pH 6 PBS before and after the addition of H_2O_2 are shown in figures 8(a) and (b), respectively. This shows one pair of well-defined redox peaks corresponding to the reversible transition of PB to prussian white [52]. Both the reduction and oxidation currents for the PPy/PB modified GEC are increased after the addition of H_2O_2. However, no electrocatalytic current can be obtained on bare GEC in the potential range scanned, indicating that the PPy/PB composite can act as a catalyst for the reduction of H_2O_2. The inset shows the change of the currents under different concentrations of H_2O_2 at −300 mV. As shown in the figure, the current increases with increasing H_2O_2 concentration. The PPy in the PPy/PB composite did not show its electrochemical activity. A possible reason is that the doping level of PPy is low or it needs many cycles to be rejuvenated. Figure 9 shows voltammograms of a PPy/Ag modified electrode. It shows a pair of strong redox peaks, corresponding to the oxidation (anions move in) and reduction (anions move out) reaction of PPy. The strong redox peaks appeared in the first cycle and retained the current intensity

after many cycles. Compared with PPy/PB, the PPy in the PPy/Ag composite shows enhanced electrochemical activity. It is well known that Ag is an important type of conductor. Although Ag nanoparticles do not make a continuous electron path, the incorporated Ag nanoparticles generate many active sites for charge transfer through the interface inside the electrode by making a good contact with the PPy matrix. The effective transport of the electrons to the electrode in the PPy/Ag matrix leads to excellent electrochemical activity. In addition, the doping level of PPy in the PPy/Ag composite is much higher than that of PPy in the PPy/PB. It is not only doped by MO but is also doped by a large amount of NO_3^-. The high doping level is beneficial for improving the electrochemical activity due to the fact that the redox reaction of PPy is moving in and out of anions. The PPy/Ag composite microtubes with enhanced electrochemical activity have potential applications in the area of controlled release.

4. Conclusion

PPy/PB and PPy/Ag composite microtubes were synthesized in one pot by using MO as a reactive self-degraded template. In contrast to reported conventional template approaches, the MO template does not need to be removed after polymerization because PPy can be doped with it during the polymerization process. Almost all of the resulting structures have a tubular-like morphology. The morphology and composition of the resulting PPy/PB and PPy/Ag composite microtubes were characterized by SEM, TEM, XRD, FTIR, and XPS. The obtained PPy/PB was immobilized on the surface of a GCE to construct a H_2O_2 biosensor. The CV measurement shows that the PPy/Ag has high electrochemical activity. The route described here is a general method to prepare composite microtubes of PPy and other inorganic materials such as Au, Pd and Ce.

Acknowledgments

This work was supported by the National Nature Science Foundation of China (Nos 20325516, 20521503), the National Basic Research Program of China (No. 2003CB615804) and the Modern Analysis Center of Nanjing University.

References

[1] Alivisatos A P 1996 *Science* **271** 933
[2] Huang J and Kaner R B 2004 *J. Am. Chem. Soc.* **126** 851
[3] Zhang Z M, Sui J, Zhang L J, Wan M X, Wei Y and Yu L M 2005 *Adv. Mater.* **17** 2854
[4] Dauginet-De Pra L and Demoustier-Champagne S 2005 *Polymer* **46** 1583
[5] Zhang X and Manohar S K 2005 *J. Am. Chem. Soc.* **127** 14257
[6] Martin C R 1994 *Science* **266** 1961
[7] Jang J and Yoon H 2003 *Chem. Commun.* 720
[8] Jang J and Yoon H 2005 *Langmuir* **21** 11484
[9] Wei Z X, Zhang Z M and Wan M X 2002 *Langmuir* **18** 917
[10] Zhang L J and Wan M X 2003 *Adv. Funct. Mater.* **13** 815
[11] Huang L, Wang Z, Wang H, Cheng X, Mitra A and Yan Y 2002 *J. Mater. Chem.* **12** 388
[12] Yan F, Xue G and Wan F 2002 *J. Mater. Chem.* **12** 2606
[13] Li L, Yan F and Xue G 2004 *J. Appl. Polym. Sci.* **91** 303
[14] Cheng D M, Xia H B and Chan H S O 2004 *Langmuir* **20** 9909
[15] Cheng D M, Zhou X D and Xia H B 2005 *Chem. Mater.* **17** 3578
[16] Huang K, Zhang Y J, Han D X, Shen Y F, Wang Z J, Yuan J H, Zhang Q X and Niu L 2006 *Nanotechnology* **17** 283
[17] An K H, Jeong S Y, Ryong H and Lee Y H 2004 *Adv. Mater.* **16** 1005
[18] Zhang W X, Wen X G and Yang S H 2003 *Langmuir* **19** 4420
[19] Lu W, Wallace G G and Karayakin A A 1998 *Electroanalysis* **10** 472
[20] Somani P and Radhakrishnan S 2002 *Mater. Chem. Phys.* **76** 15
[21] Buschmann W E, Ensling J, Gutlich P and Miller J S 1999 *Chem. Eur. J.* **5** 3019
[22] Mortimer R J and Warren C P 1999 *J. Electroanal. Chem.* **460** 263
[23] Honda K and Hayashi H 1987 *J. Electrochem. Soc.* **134** 1330
[24] Ricci F, Amine A, Palleschi G and Moscone D 2003 *Biosen. Bioelectron.* **18** 165
[25] Raitman O A, Katz E, Willner I, Chegel V I and Popova G V 2001 *Angew. Chem. Int. Edn* **40** 3649
[26] Huang K, Zhang Y, Long Y, Yuan J, Han D, Wang Z, Niu L and Chen Z 2006 *Chem. Eur. J.* **12** 5314
[27] Majumdar G, Goswami M, Sarma T K, Paul A and Chattopadhyay A 2005 *Langmuir* **21** 1663
[28] Zhao H, Yuan Y, Adeloju S and Wallace G G 2002 *Anal. Chim. Acta* **472** 113
[29] Garjonyte R and Malinauskas A 2000 *Sensors Actuators* B **63** 122
[30] Pillalamarri S K, Blum F D, Tokuhiro A T and Bertino M F 2005 *Chem. Mater.* **17** 5941
[31] Chen A, Kamata K, Nakagawa M, Iyoda T, Haiqiao W and Li X 2005 *J. Phys. Chem.* B **109** 18283
[32] Pinter E, Patakfalvi R, Fulei T, Gingl Z, Dekany I and Visy C 2005 *J. Phys. Chem.* B **109** 17474
[33] Koncki R and Wolfbeis O S 1998 *Anal. Chem.* **70** 2544
[34] Yang X, Zhu Z, Dai T and Lu Y 2005 *Macromol. Rapid Commun.* **26** 1736
[35] Quadrifoglio F and Crescenzi V 1971 *J. Colloid Interface Sci.* **35** 447
[36] Talens-Alesson F I, Anthony S and Bryce M 2004 *Water Res.* **38** 1477
[37] Qian R Y, Pei Q B and Huang Z T 1991 *Macromol. Chem.* **192** 1263
[38] Ikeda O and Yoneyama H 1989 *J. Electroanal. Chem.* **265** 323
[39] Busher H J, Schwarzenbach D, Petter W and Ludi A 1977 *Inorg. Chem.* **16** 2704
[40] Gao Y *et al* 2004 *J. Phys. Chem.* B **108** 12877
[41] Kojima Y, Usuki A A, Kawasumi M, Okada A, Kurauchi T and Kamigaito O 1993 *J. Polym. Sci.* A **31** 983
[42] Seo I, Pyo M and Cho G 2002 *Langmuir* **18** 7253
[43] Chen A, Wang L and Li X 2004 *Chem. Commun.* **14** 1863
[44] Henry M C, Hsueh C C and Timko B P 2001 *J. Electrochem. Soc.* **148** 155
[45] Lee D K, Lee S H and Char K 2000 *Macromol. Rapid Commun.* **21** 1136
[46] Zhang Z P, Zhang L D and Wang S X 2001 *Polymer* **42** 8315
[47] Cho G, Fung B M, Glatzhofer D T, Lee J S and Shul Y G 2001 *Langmuir* **17** 456
[48] Jang J and Oh J H 2005 *Adv. Funct. Mater.* **15** 494
[49] Mathis G I and Troung V T 1997 *Synth. Met.* **89** 103
[50] Ayers J B and Piggs W H 1971 *J. Inorg. Nucl. Chem.* **33** 721
[51] Wilde R E, Ghosh S N and Marshall B J 1970 *Inorg. Chem.* **9** 2512
[52] Delongchamp D M and Hammond P T 2004 *Adv. Funct. Mater.* **14** 224
[53] Lisowska-Oleksiak A, Nowak A P and Jasulaitiene V 2006 *Electrochem. Commun.* **8** 107
[54] Tan K L, Tan B T G, Kang E T, Neoh K G and Ong Y K 1990 *Phys. Rev.* B **42** 7563